

Provided for non-commercial research and education use.
Not for reproduction, distribution or commercial use.



This article appeared in a journal published by Elsevier. The attached copy is furnished to the author for internal non-commercial research and education use, including for instruction at the authors institution and sharing with colleagues.

Other uses, including reproduction and distribution, or selling or licensing copies, or posting to personal, institutional or third party websites are prohibited.

In most cases authors are permitted to post their version of the article (e.g. in Word or Tex form) to their personal website or institutional repository. Authors requiring further information regarding Elsevier's archiving and manuscript policies are encouraged to visit:

<http://www.elsevier.com/copyright>



Contents lists available at ScienceDirect

Physics Letters A

www.elsevier.com/locate/pla



Correlation between microstructure and first-order magnetization reversal in the $\text{SmCo}_5/\alpha\text{-Fe}$ nanocomposite magnets

Chuan-bing Rong^{a,*}, Ying Zhang^b, M.J. Kramer^b, J. Ping Liu^{a,*}

^a Department of Physics, University of Texas at Arlington, Arlington, TX 76019, USA

^b Division of Materials Science and Engineering, Ames Laboratory, USDOE, Iowa State University, Ames, IA 50011, USA

ARTICLE INFO

Article history:

Received 9 November 2010
 Received in revised form 27 January 2011
 Accepted 2 February 2011
 Available online 3 February 2011
 Communicated by R. Wu

Keywords:

First-order reversal curve
 Nanocomposite magnets
 Magnetostatic and intergranular exchange interactions

ABSTRACT

$\text{SmCo}_5/\alpha\text{-Fe}$ nanocomposite magnets with different morphology have been fabricated by ball milling of the micrometer sized SmCo_5 and $\alpha\text{-Fe}$ powders. The $\alpha\text{-Fe}$ grains vary from elongated nano-strips to spherical nanoparticles with increasing milling time. The inter-phase exchange coupling is enhanced with increasing milling time due to reduced grain size. The first-order reversal curves (FORCs) are taken to identify optimal conditions for exchange coupling. It has been found that the stripped morphology results in weak inter-phase exchange coupling, while enhanced exchange coupling is observed with further reduction of the soft-phase grain size. Compared with the measurement of demagnetization curves, FORC analysis provides more information on the magnetostatic as well as the exchange interactions.

© 2011 Elsevier B.V. All rights reserved.

1. Introduction

Exchange-coupled nanocomposite magnets containing magnetically hard and soft phases with optimal nanoscale morphology and composition distribution will have extremely high energy products [1–3]. The prerequisite for the effective inter-phase exchange coupling is homogenous distribution of the soft phase with grain size smaller than a critical size. Obviously, the magnetic properties and magnetization reversal processes are directly related to morphology of the composite materials. The experimental and theoretical studies on the correlations between microstructure (such as grain size and soft-phase content) and magnetic properties as well as the magnetization reversal behavior have been reported extensively [4–10]. Recently, we fabricated $\text{SmCo}_5/\alpha\text{-Fe}$ nanocomposite magnets with $\alpha\text{-Fe}$ grain size about 10 nm by ball milling of micrometer-sized Sm-Co and $\alpha\text{-Fe}$ powders [11,12]. It was found that the morphology of the $\alpha\text{-Fe}$ grains evolved with the ball milling time. Initially wide strips of $\alpha\text{-Fe}$ grains formed after short time of milling. The strips were then thinned like Ramen (extended noodles) and eventually broken into spherical nanometer sized grains upon further ball milling. In this work, we examine the effect of the morphology on the magnetization reversal processing of the SmCo_5/Fe composite system by measuring the first-order reversal curves (FORC). The magnetostatic and exchange interactions between the magnetically hard and soft phases can be

mapped using FORC diagrams, which are plotted by probing the interior of a hysteresis loop with multiple FORCs.

2. Experiments

The raw materials of SmCo_5 ($\sim 45 \mu\text{m}$) and $\alpha\text{-Fe}$ ($\sim 10 \mu\text{m}$) were mixed with a weight ratio of 20% Fe and ball milled in a SPEX M8000 machine with a container made of 440C hardened steel. The weight ratio of sample to ball is around 1 : 30. The milling-time was varied from 0.5 to 10 hours. The powders were then annealed at 525 °C for 30 minutes to develop the appropriate crystalline structure. The morphology and crystalline structure were characterized by transmission electron microscopy (TEM), Energy-Filtered TEM (EFTEM), and X-ray diffraction (XRD) using $\text{Cu } K_{\alpha}$ radiation. Magnetic properties were measured with superconducting quantum interference device (SQUID) magnetometer with a maximum applied field of 60 kOe. The samples for magnetic measurement were prepared by fixing the powders with epoxy resin.

A FORC measurement begins by saturating the samples with a large positive applied field. The field is decreased to a reversal field (H_r), and then the FORC is defined as the magnetization curve measured with increasing applied field (H_a) back to saturation. The measurement procedure is repeated for different values of reversal fields to obtain a suite of FORCs and a two-dimensional distribution function. The FORC diagram is defined as the mixed second derivative of the applied field and the reversal field. When a FORC distribution is plotted, it is convenient to change coordinates from $\{H_r, H_a\}$ to $\{H_u = (H_a + H_r)/2, H_c = (H_a - H_r)/2\}$. A detailed description of FORC distribution can be found in Refs. [13–15].

* Corresponding authors.

E-mail addresses: rong@uta.edu (C.B. Rong), pliu@uta.edu (J.P. Liu).

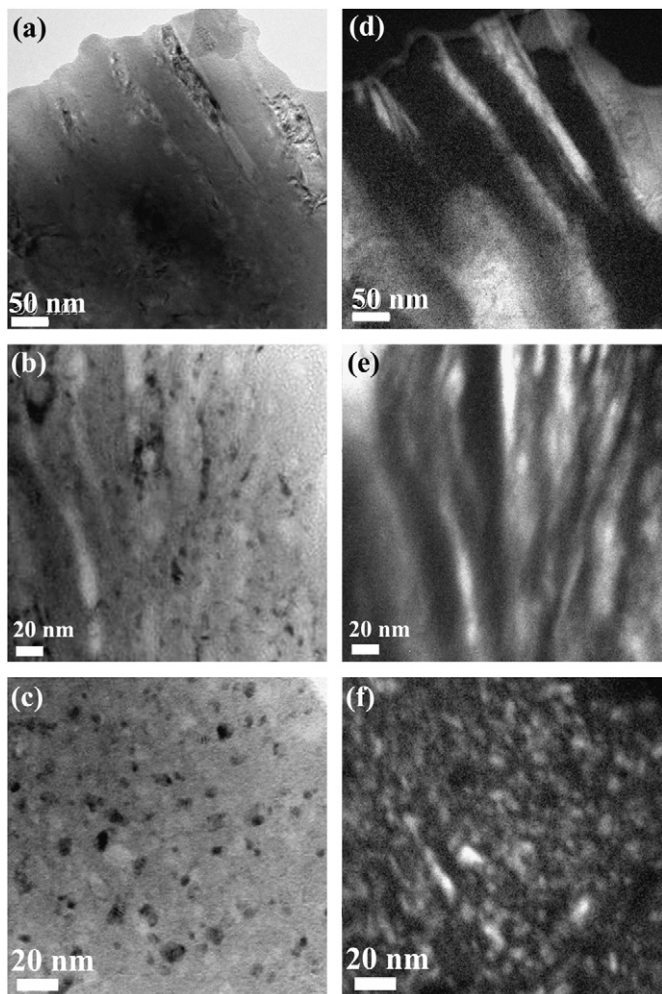


Fig. 1. Bright field TEM image of (a) 30, (b) 60 and (c) 240 minutes ball milled SmCo/Fe after annealing at 525 °C for 30 minutes; and EFTEM mappings showing Fe distributions in the samples after ball milled (d) 30 min, (e) 60 min and (f) 240 min, respectively. The bright areas represent Fe-rich in the EFTEM images.

It should be mentioned that the FORC distribution in this work only represents the contribution from the irreversible magnetization switching. The FORCs are measured in SQUID magnetometer and the diagrams are calculated using the software FORCinel in this work [16]. We did not consider demagnetization factor when the FORC diagram was calculated.

3. Results and discussion

Fig. 1 shows the bright-field TEM images and EFTEM Fe mappings of the two-phase systems with different ball-milling time. The higher brightness in the EFTEM image corresponds to higher concentrations of Fe. Starting with raw α -Fe powders of nearly $\sim 10 \mu\text{m}$ spherical particles, the soft magnetic phase grains were stretched and elongated after 30 minutes of ball milling, as seen from Figs. 1(a) and (d). Extending the milling time to 60 minutes resulted in thinner α -Fe strips, as shown in Figs. 1(b) and (e). With further milling, the nanoscale α -Fe strips began to break up into isolated equiaxed nanoscale grains. After 240 minutes of milling, a homogenous distribution of the soft phase grains was obtained, with the soft phase embedded in the hard-phase matrix, as shown in Figs. 1(c) and (f). The evolution of this microstructure may be explained by the brittle-ductile two-phase deformation behavior since the SmCo₅/Fe system is a mechanically brittle/ductile system [11].

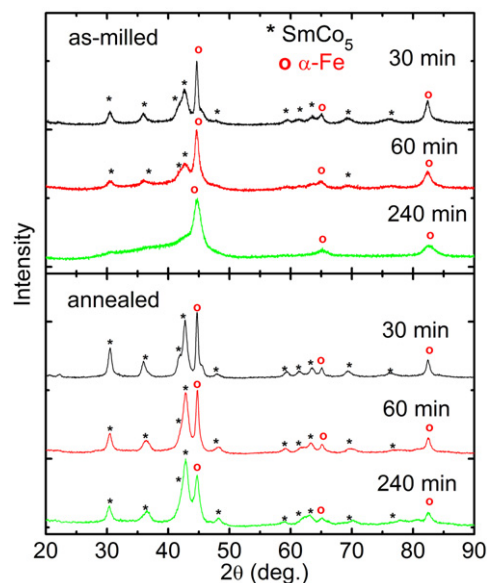


Fig. 2. XRD patterns of the (a) as-milled and (b) annealed powders of the 30, 60 and 240 minutes milled powders. The annealing condition is 525 °C for 30 minutes.

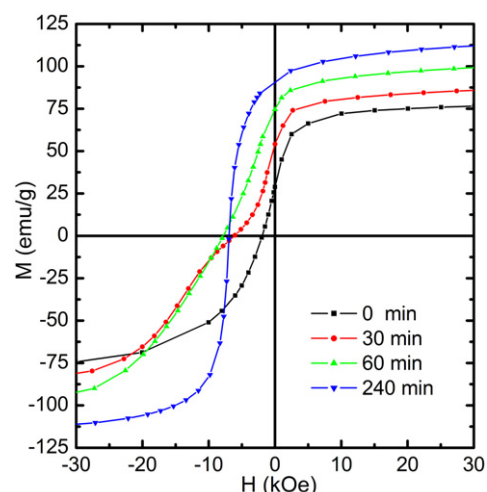


Fig. 3. Demagnetization curves of the powders without milling and milled for 30, 60 and 240 minutes after annealing at 525 °C for 30 minutes.

High energy ball milling processing usually leads to amorphization, which occurred for the SmCo₅ phase in this investigation [17]. Fig. 2(a) shows the XRD patterns of the as-milled powders after 30, 60 and 240 minutes ball milling. It was found that the peaks of both the Sm–Co and α -Fe phases are broadened with milling time, indicating a grain size reduction. The Sm–Co phase becomes amorphous when the milling time is longer than 240 minutes. A post-annealing treatment is therefore necessary to develop the desired crystalline structures with hard magnetic properties while retaining the nanoscale grain size of the soft phase. Our experiments showed that an optimized annealing (crystallization) condition is 525 °C for 30 minutes. As one can see in Fig. 2(b) that the crystallized SmCo₅ phase forms after being annealed for all samples. Most importantly, the grain size of SmCo₅ and α -Fe phases are only about 12 nm for the powders milled for 240 minutes and after annealing, determined by the Williamson–Hall analysis. The size of the magnetically soft phase is very close to the critical dimension of effective exchange coupling, which is determined by the hard-phase domain wall thickness and soft-phase magnetic properties [1–3,18]. Without grain size reduction through

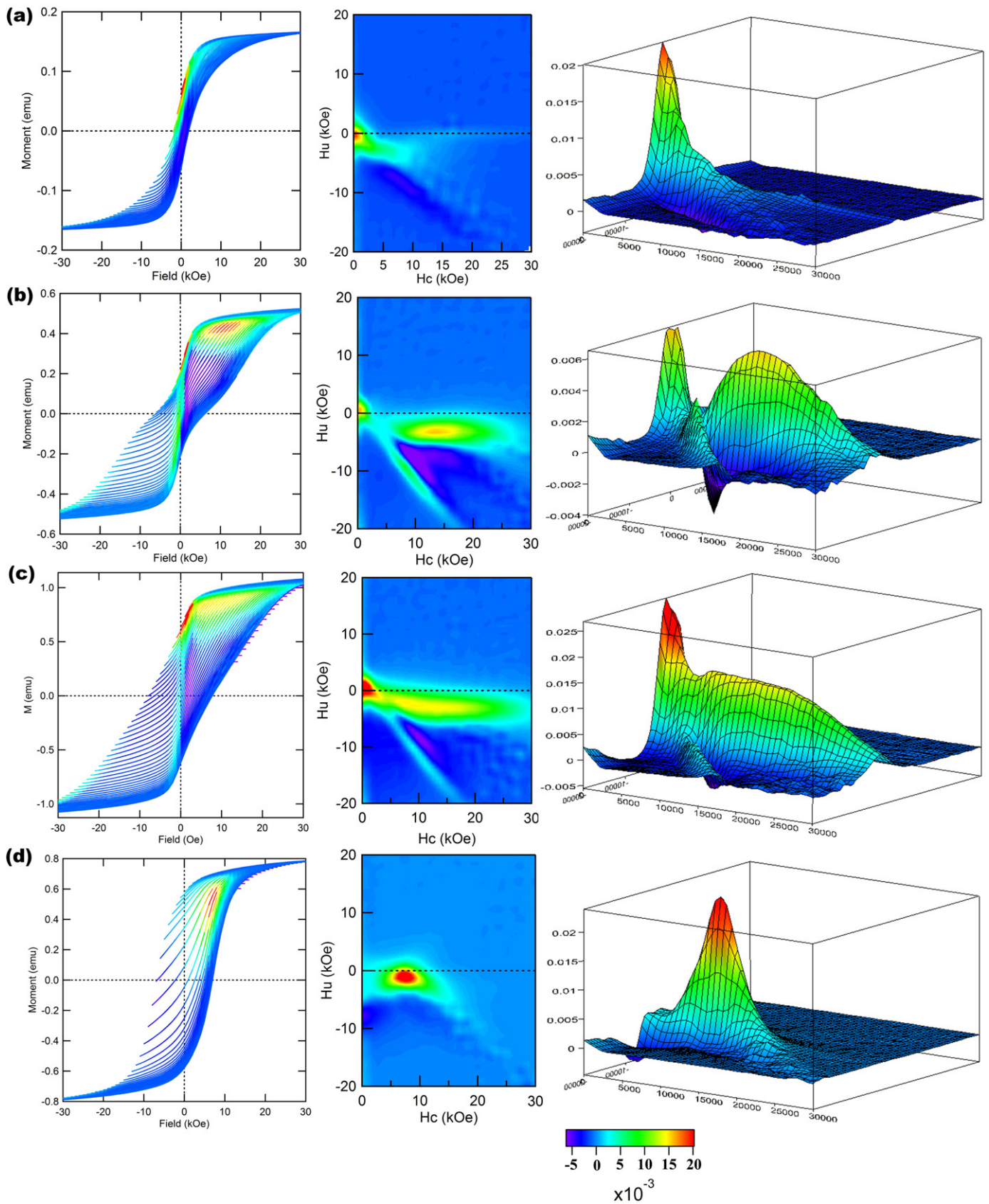


Fig. 4. The 2D and 3D FORC diagrams of the samples (a) without milling, and milled for (b) 30, (c) 60, and (d) 240 minutes after annealing at 525 °C for 30 minutes. Left column is the colored FORC curves with the FORC distribution plotted inside the hysteresis loop. The middle column is the two-dimensional FORC diagrams and right column is three-dimensional FORC diagrams.

ball milling, the soft magnetic phase would be too large for effective exchange coupling, such as in samples milled for 30 and 60 minutes.

Fig. 3 shows the demagnetization curves of the annealed $\text{SmCo}_5 + 20 \text{ wt}\% \alpha\text{-Fe}$ powders milled for different time. The demagnetization curve of the mixture without milling is also given in Fig. 3 for comparison. It is found that coercivity of the mixture without milling is very small because of the very large grain size of SmCo_5 phase. For samples milled for 30 and 60 minutes there is a noticeable kink on the demagnetization curves, implying a decoupled two-phase demagnetization behavior because the soft-phase grains are too large to be effectively exchange coupled by the hard phase. Sample milled for 240 minutes has smooth demagnetization curve, consistent with the uniform nanoscale morphology.

Fig. 4 presents the 2D and 3D FORC diagrams of the powders milled for 30, 60, and 240 minutes after annealing. The FORC diagrams of the mixture without milling are also given for comparison. The correlation between FORC distribution and the microstructure of the composite magnets has been described and discussed as follows:

- As one can see that there is only one major peak around the origin for the un-milled sample since both the raw $\alpha\text{-Fe}$ and SmCo_5 powders have low coercivity.
- Ball milling reduces the grain size while post annealing restores the crystallinity for the SmCo_5 phase, which in turn raises the coercivity. As a result, there are two completely separated peaks along the bias axis, $H_u = 0$, for the sample milled 30 minutes, one around origin and one around 15 kOe, which represent the magnetization reversals of the magnetically soft and hard phases, respectively. The separated magnetization reversal indicates weak exchange interaction between the two magnetic phases. More interestingly, a distinct ridge is observed at an angle of $\sim 135^\circ$ across the lower half of the FORC diagram (Fig. 4(b)), which could be attributed to the magnetostatic interaction between the magnetically soft and hard phases, predicted by simple models of FORC distribution [19,20].
- The two peaks along the bias axis merge when milling time is increased to 60 minutes. This could be attributed to the grain refinement of $\alpha\text{-Fe}$ phase. The magnetic moments in the $\alpha\text{-Fe}$ grains are partially exchange-coupled and thus the switching field of the magnetically soft phase increases. However, a large amount of $\alpha\text{-Fe}$ phase is still in a form of strips as shown in Fig. 1(c), therefore there is still a strong peak around the origin in the FORC diagram. In addition, the ridge around $\sim 135^\circ$ becomes weak with increasing milling time since the exchange interaction starts to dominate the magnetization behavior with grain refinement.
- Extending milling time leads to further grain refinement and homogeneously distributed $\alpha\text{-Fe}$ grains are obtained when the milling time is longer than 4 hours. As one can see in Fig. 4(d) that the soft phase is completely exchange coupled and thus there is only one major peak in the FORC diagram around $H_c = 8 \text{ kOe}$. The magnetization reversal happens simultaneously in both hard and soft magnetic phases, i.e.,

a single-phase magnetization reversal behavior is observed in the nanocomposite SmCo_5/Fe system with homogeneously distributed magnetic soft phase.

4. Conclusions

In summary, the nanoscale morphology of the $\text{SmCo}_5/\alpha\text{-Fe}$ nanocomposite magnets evolves with ball milling. The soft phase grains change their morphology in a way similar to extended noodles and eventually break into nanometer sized spherical grains upon further milling. The first-order reversal curves were used to monitor the inter-phase magnetostatic and exchange interactions. It has been found that the stripped microstructure with large magnetic soft grains results in weak inter-phase exchange coupling but strong magnetostatic interaction. With continuing refining of soft-phase grains, the inter-phase exchange coupling is enhanced as observed from the FORCs, which results in improved squareness in demagnetization curves, and thus increased energy product.

Acknowledgements

This work has been supported in part by the US Office of Naval Research/MURI project under grant N00014-05-1-049, US DoD/DARPA/ARO under grant W911NF-08-1-0249, and by the University of Texas-Arlington. The microscopy was performed at the Ames laboratory which is supported in part by the US Department of Energy, Office of Basic Energy Science, under contract DE-AC02-07CH11358.

References

- R. Skomski, J.M.D. Coey, Phys. Rev. B 48 (1993) 15812.
- T. Schrefl, H. Kronmüller, J. Fidler, J. Magn. Magn. Mater. 127 (1993) L273.
- C.B. Rong, H.W. Zhang, R.J. Chen, S.L. He, B.G. Shen, J. Magn. Magn. Mater. 302 (2006) 126.
- H.A. Davies, J. Magn. Magn. Mater. 157 (1996) 11.
- Z. Wang, S. Zhou, M. Zhang, Y. Qiao, J. Appl. Phys. 88 (2000) 591.
- R. Fischer, T. Schrefl, H. Kronmüller, J. Fidler, J. Magn. Magn. Mater. 150 (1995) 329.
- R. Fischer, T. Schrefl, H. Kronmüller, J. Fidler, J. Magn. Magn. Mater. 153 (1996) 35.
- R. Fischer, T. Leineweber, H. Kronmüller, Phys. Rev. B 57 (1998) 10723.
- Y. Choi, J.S. Jiang, J.E. Pearson, S.D. Bader, J.P. Liu, Appl. Phys. Lett. 91 (2007) 022502.
- C.B. Rong, J.P. Liu, Appl. Phys. Lett. 94 (2009) 172510.
- C.B. Rong, Y. Zhang, N. Poudyal, X.Y. Xiong, M.J. Kramer, J.P. Liu, Appl. Phys. Lett. 96 (2010) 102513.
- Y. Zhang, M.J. Kramer, C.B. Rong, J.P. Liu, Appl. Phys. Lett. 97 (2010) 032506.
- C.R. Pike, A.P. Roberts, K.L. Verosub, J. Appl. Phys. 85 (1999) 6660.
- A.P. Roberts, C.R. Pike, K.L. Verosub, J. Geophys. Res. 105 (2000) 28461.
- R.K. Dumas, C.P. Li, I.V. Roshchin, I.K. Schuller, K. Liu, Phys. Rev. B 75 (2007) 134405.
- R.J. Harrison, J.M. Feinberg, Geochemistry Geophysics Geosystems 9 (2008) 1.
- J. Zhang, S.Y. Zhang, H.W. Zhang, B.G. Shen, J. Appl. Phys. 89 (2001) 5601.
- J.P. Liu, in: J.P. Liu, E. Fullerton, O. Gutfleisch, D.J. Sellmyer (Eds.), Nanoscale Magnetic Materials and Applications, Springer, New York, 2009, p. 316.
- G. Acton, K.L. Verosub, A. Roth, D. Linderholm, Eos Trans. AGU 86(52), Fall Meeting Suppl., Abstract GP13A-0044.
- G. Acton, Q.Z. Yin, K.L. Verosub, L. Jovane, A. Roth, B. Jacobsen, D.S. Ebel, J. Geophys. Res. 112 (2007) B03S90.